Security and Safety, Vol. 2, 2023015 (2023)

Security and Safety in Physical Layer Systems

Research Article

Open Access

Information Network

Covert communication in relay and RIS networks

Jinsong Hu[1,2,*], Xiaoqiang Shi[1,2], Youjia Chen[1,2,*], Tiesong Zhao[1,2], and Feng Shu[3]

[1] *College of Physics and Information Engineering, Fuzhou University, Fuzhou, Fujian 350116, China*
[2] *Fujian Key Laboratory for Intelligent Processing and Wireless Transmission of Media Information, Fuzhou University, Fuzhou, Fujian 350116, China*
[3] *School of Information and Communication Engineering, Hainan University, Haikou, Hainan 570100, China*

Received: 21 December 2022 / Revised: 10 March 2023 / Accepted: 14 June 2023 / Published online: 03 July 2023

Abstract Covert communication aims to prevent the warden from detecting the presence of communications, *i.e.* with a negligible detection probability. When the distance between the transmitter and the legitimate receiver is large, large transmission power is needed, which in turn increases the detection probability. Relay is an effective technique to tackle this problem, and various relaying strategies have been proposed for long-distance covert communication in these years. In this article, we first offer a tutorial on the relaying strategies utilized in covert transmission. With the emergence of reflecting intelligent surface and its application in covert communications, we propose a hybrid relay-reflecting intelligent surface (HR-RIS)-assisted strategy to further enhance the performance of covert communications, which simultaneously improves the signal strength received at the legitimate receiver and degrades that at the warden relying on optimizing both the phase and the amplitude of the HR-RIS elements. The numerical results show that the proposed HR-RIS-assisted strategy significantly outperforms the conventional RIS-aided strategy in terms of covert rate.

Keywords Covert communication, relay, reflecting intelligent surface

Citation Hu J, Shi X and Chen Y et al. Covert communication in relay and RIS networks. Security and Safety 2023; **2**: 2023015. https://doi.org/10.1051/sands/2023015

1 Introduction

Security and privacy are two critical issues in current communication systems. The development of classical cryptography, information-theoretic security, and quantum cryptography have greatly improved the security levels of data transmission. Cryptography presents the adversary with a problem that it is assumed not to be able to solve because of computational constraints, while information-theoretic security presents the adversary with a signal from which no information can be extracted. They addressed many security issues by protecting the content of the message, they cannot mitigate the threat of communication detection. Adversary/warden detects a potential data transmission, it may disturb it. To tackle this issue, covert communication arose, which focuses on transmitting the confidential information from a transmitter to legitimate receivers, while avoiding being detected by the potential warden [1, 2].

For instance, the transmitter Alice tends to transmit a confidential message to the receiver Bob with in the presence of warden Willie. That is, Alice has to provide a reliable transmission to Bob while the transmission remains hidden from Willie. Willie, on the other hand, is not interested in the content of the message and only wants to determine whether Alice transmits any message to Bob or not. We note that this is in strong contrast to the role of an eavesdropper in traditional physical layer security schemes where

the eavesdropper is aware of the presence of a message transmission and looks to decode the information transmitted from Alice to Bob.

Consequently, while Bob has to decode the information sent by Alice, Willie has to confront a detection problem, attempting to distinguish between the two potential states of Alice's transmission. Recent research efforts in the domain of covert communications have explored different problems in this field, from establishing the achievable fundamental limits to exploiting any uncertainties at the potential adversary Willie, including noise, channel, network interference, and jamming signals/artificial noise introducing uncertainties in Willie's observations.

Noise uncertainty: The lack of knowledge of the exact noise power is called noise uncertainty. In practice, the sources of background noise include thermal noise, quantization noise, imperfect filters, *etc.* Noise uncertainty is almost unavoidable due to, *e.g.*, temperature change, environmental noise change, and calibration error. Therefore, the consideration of noise uncertainty is practical and necessary for the study related to power detection. The authors in [3] considered two models of noise uncertainty at the Willie, *i.e.*, the bounded uncertainty model and the unbounded uncertainty model. In [4], the noise uncertainty is used to analyze the minimum error detection probability of the warden to realize covert wireless communication in space-air-ground integrated vehicular networks. Considering the noise uncertainty at warden, the authors in [5] studied the IoT covert communication network with the channel state information (CSI) unawareness at Bob.

Channel uncertainty: All the node experience uncertainty about their channel knowledge. One of the main assumptions in most covert communications literature is that the CSI of both the covert link is perfectly known by both the legitimate receiver and the transmitter. Usually, the CSI is obtained at the receiver by channel estimation during pilot transmission. Then, a feedback link (if available) is used to send the CSI to the transmitter. Hence, the accuracy of the channel estimation at the receiver affects the quality of CSI at the transmitter. However, in covert communication scenarios, transmitting pilots and acquiring feedback is often infeasible, especially as the transmission of pilots will also enable the adversary to acquire channel information from the covert transmitter. The authors in [6] considered the scenario where a public link is used to hide a cover link while users including the legitimate receiver and warden Willie suffer from uncertainty in their channel knowledge from the transmitter. Under the CSI uncertainty scenario, Willie's optimal detection performance is derived and then the optimal transmission rates are determined for both the legitimate and covert links under certain transmission outage probabilities. In [7], the authors analyzed the ability of the suspicious receiver to detect the artificial noise under the channel uncertainty and optimized the performance of the covert surveillance performance.

Interference: In practical wireless networks, a major source of the uncertain interference at the receiver is the ambient signals from other transmitters, and the uncertainty of the aggregate received interference at the warden will help to achieve the positive covert throughput in covert communications. The uncertainty of the aggregated interference experienced by the warden is beneficial to the potential transmitters for covert communication [8]. The authors in [9] studied covert communication in wireless networks with the aid of stochastic geometry. Instead of assuming that all communication nodes in the network are friendly helpers, it is assumed that all nodes in the network, which are distributed according to a homogeneous Poisson point process (PPP), randomly transmit without the intention to help the covert communication. When the interference is sufficiently small and comparable with the receiver noise, the covert throughput increases as the density or the transmit power of the concurrent interferers increases. The authors of [10] derived the exact covert capacity region in the covert communication network and proved that the scheme using interference as noise is optimal.

Jamming signals/artificial noise: The performance of covert communication can be improved by letting a friendly jammer deliberately broadcast a jamming signal to degrade the detection performance of the adversary. If this jammer randomly varies its transmit power appropriately or if time-varying multipath fading causes sufficient variation, channel estimation during periods outside the period time when Willie is attempting to detect Alice's transmission cannot be used to estimate the statistics of the noise impacting Willie's receiver during the period of interest [11]. The authors consider the use of an FD receiver to achieve covert communication [12]. Specifically, the full-duplex (FD) receiver generates AN with a randomized transmit power, causing deliberate confusion and affecting the decisions at Willie regarding the presence of any covert transmissions. The use of an FD receiver generating AN provides a cover for covert transmission and offers a multitude of benefits as compared to the use of a separate, independent jammer. Being equipped with an FD receiver, we can exercise better control over the power

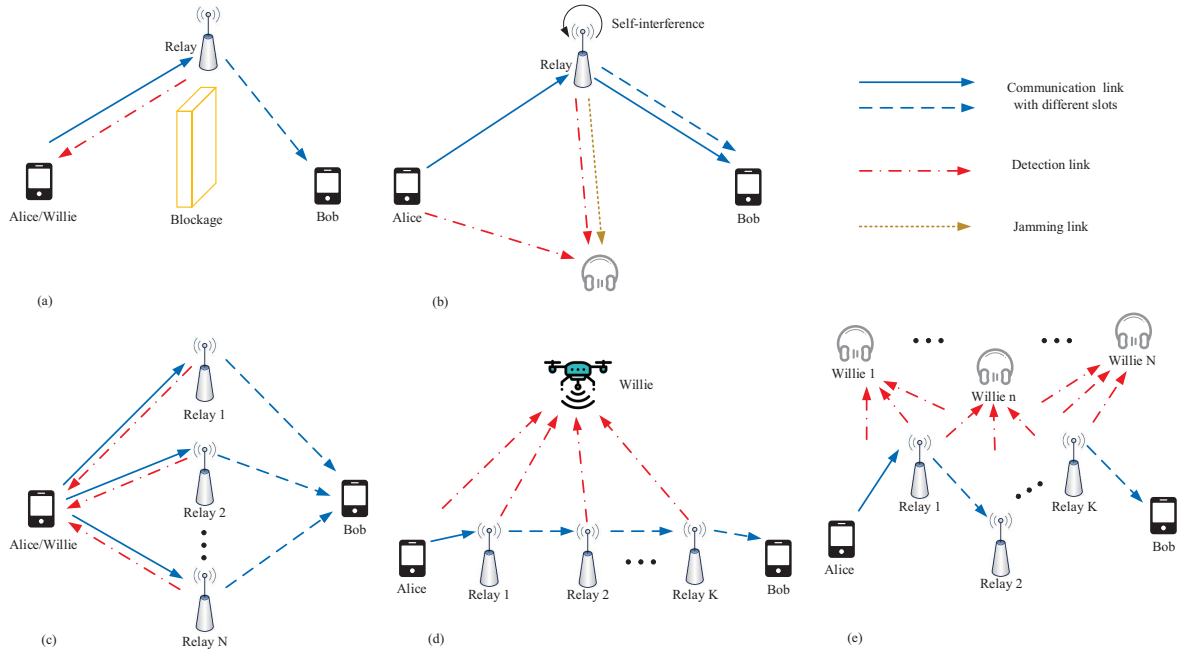

Figure 1. Typical applications of relay network in covert communication systems: a) Greedy relay with blockage; b) Relay with different duplex mode; c) Relay networks with relay selection ; d) Multi-Hop against UAV surveillance; e) Multi-Hop against multiple collaborating Willies

used for transmitting AN, hence better management of system resources to achieve a higher covert rate. Furthermore, while Willie will face strong interference, the self-interference at the FD receiver can be greatly suppressed by the well-developed self-interference cancellation techniques. Furthermore, a finite block-length covert communication scheme with artificial noise was proposed in [13]. In [14], the authors investigated the influence of the jammer equipped with multiple antennas on Alice's transmit power, and consequently on covert communication performance. The authors in [15] adopted the channel inversion power control to maintain the received power with a constant value for covert communication, while the receiver sends the full-duplex artificial noise with random power, which allows the transmitter to ensure security with higher transmit power.

The aforementioned contributions are mainly focused on improving wireless covertness without paying much attention to communication reliability. When Alice and Bob are located far from each other, in order to make the probability of error at Bob sufficiently small, Alice should use a high transmit power. However, this increases the probability of being detected by Willie, especially if Willie is close to Alice and thus receives a strong signal. The point-to-point covert communication in the presence of a single warden that is discussed in the literature should be extended to scenarios with multiple receivers (hops) for relaying the covert message.

2 Typical applications of relay for covert communications

The following discussions will show that the covertness of relay-assisted networks can be enhanced by exploiting the distributed diversity and shortening the access distance with the relay. Figure 1 shows several typical scenarios of relay-assisted covert communications. The existing research works on the relay in covert communications are demonstrated to show how to achieve the demands of long-distance wireless communication with low detection probability and reliable transmission.

2.1 Greedy relay with blockage

As shown in Fig. 1a, a one-way relay network over a Rayleigh fading channel is considered, in which the source transmits information to the destination with the aid of the relay, since a direct link from

source to destination is not available [16]. In the considered scenario, the source allocates some resources (*e.g.*, power [17] and spectrum) to relay in order to seek its help to relay the message to the destination. However, in some scenarios, the relay may intend to use this resource to transmit its message to a destination as well, which is forbidden by the source and thus should be kept covert from the source. As such, in the considered system model the source is also the warden which is detecting whether the relay transmits its information to the destination when it is aiding the transmission from the source to the destination. The covert transmission from the relay to the destination is similar to steganography, in which covert information is transmitted by hiding in innocuous objects. These innocuous objects are utilized as "cover medium" to carry the covert information. In [16] and [17], the innocuous objects are the forwarding transmissions from relay to the destination. The main difference between this work and steganography is that in this work the covert information is shielded by the forwarding transmissions from the relay to the destination at the physical layer, while in steganography the covert information is hidden and transmitted by encoding or modifying some contents (*e.g.*, shared videos or images) at the application layer. The covert communication from a relay to a destination only occurs when the successful transmission from source to destination is guaranteed. As such, when the covert message is transmitted via the relay, successive interference cancellation (SIC) that allows a receiver to decode different signals arriving simultaneously is implemented at the destination. Following SIC, the destination decodes the stronger signal (*i.e.*, original message) first, subtracts it from the combined signal, and finally decodes the weaker one (*i.e.*, covert message) from the residue. More recently, the authors in [18] proposed two covert transmission schemes, named random beamforming and maximum-ratio transmission (MRT) beamforming to guarantee reception reliability at the destination, when the greedy relay is equipped with multiple antennas.

2.2 Relay with different duplex mode

Figure 1b illustrates that the relay can work in either the full-duplex (FD) mode or the half-duplex (HD) mode [19]. Under the FD mode, the relay can simultaneously receive and forward information on the same channel, but the communication is negatively affected by the self-interference of the Relay. Under the HD mode, Relay receives and forwards information to users at two orthogonal time slots, which experience two phases. Therefore, the relay to flexibly switch between the FD and HD modes for improving the covert rate performance, and optimize the relay transmit power to achieve the covert rate maximization under such a joint mode. It is worth noting that Relay always sends the jamming signal to Willie when Alice does not transmit. Under the FD mode, although suffering from self-interference, can also enhance the covert rate by careful power control. As for the HD mode, it can avoid the negative effect of self-interference. However, it may reduce the covert rate due to the different receiving and forwarding time slots at the relay.

2.3 Relay networks with relay selection

In multiple-relay networks, relay selection has been regarded as an effective technique to achieve spacial diversity gain. In [20], a covert transmission scheme in a relay selection system was proposed, where the relay with the best relay-to-destination link is selected to forward the information, it can also opportunistically transmit its message covertly to the destination, which is shown in Fig. 1c. This relay network consists of one source, one destination, and multiple decode-and-forward (DF) relays. When forwarding the source's message, the selected relay decodes the data received in the first phase, encodes them with another codebook, and then transmits them to the destination. Hence, the received SNR at the relay decides the success of decoding. The authors in [20] investigated the trade-off between covertness and reliability in multiple relay systems, where the probability of detection error (*i.e.*, covertness) is quantified in terms of the probability that the warden fails in detecting the power relay's covert signal, while reliability represents the probability that an outage event is encountered at the relay for decoding the original message. This work showed that the diversity gain provided by relay selection will lead to a decrease in the probability of detection error.

Table 1. Typical Applications of relay for Covert Communications

Ref	Main feature	Roles of relay
[16, 17]	Relay transmits covert information to the destination on top of forwarding the source's message.	Amplify-and-forward the original message and superpose the covert information on the existing communication.
[19]	Relay can flexibly choose the FD or the HD mode.	Amplify-and-forward the covert information and send jamming signal to disturb Willie.
[20]	The relay-to-destination link is selected to forward the information.	Decode-and-forward the original message and superpose the covert information on the existing communication.
[21]	Linear multi-hop relaying network is monitored by UAV.	Decode-and-forward the covert information.
[22]	Multi-hop covert communication find optimal routing under multiple collaborating Willies' surveillance.	Decode-and-forward the covert information with a single key or independent keys.

Note: This is text of the table footnotes.

2.4 Multi-Hop against UAV's surveillance

As shown in Fig. 1d, the authors in [21] considered an unmanned aerial vehicle (UAV) in the air to act as a warden to monitor any covert communication and an eavesdropper to wiretap the transmitted signal. Compared with the terrestrial channels, the characteristics of the air-to-ground channels make legitimate information particularly vulnerable to being detected and wiretapped. Compared with the terrestrial channels, the advantages of the air-to-ground channels lead to the proneness of legitimate information leakage and detection. In order to reduce the information leakage for a pair of terrestrial nodes against the UAV surveillance while maximizing the throughput, the optimal designs of coding rate, transmission power, and the number of hops are exploited in this work. This strategy is especially suitable for networks with limited energy and long-distance between the source and the destination.

2.5 Multi-Hop against multiple collaborating willies

In covert communication, when the distance between Alice and Bob becomes large compared with the distance between Alice and Willie(s) shown in Fig. 1e, the performance of covert communication degrades. In this case, multi-hop transmission via intermediate relays can help to improve performance. The multi-hop covert communication over a moderate-size network and in the presence of multiple collaborating Willies is studied in [22]. For covert communication, the source and the intermediate relays use a key to encode the message. The relays can transmit covertly using either a single key for all relays or different independent keys at the relays. The routing algorithms for maximizing the covert throughput and minimizing the end-to-end delay are developed for two relaying approaches.

3 Intelligent reflecting surface assisted covert communication

Since the relay forwards signals to assist source-destination transmission in an active mode, leading to a high power consumption problem when compared with the RIS. In addition, the amplifying noise at the amplify-and-forward (AF) relay will increase the probability of being detected at Willie and the reduction of the signal-to-noise ratio at the DF relay will lead to a higher decoding error probability.

As a special kind of relay, the authors in [23] presented the potential of using the intelligent reflecting surface (IRS), also known as reflecting intelligent surface (RIS), to improve covert communication performance. In this section, we propose a case study of RIS to assist the signal transmission from source to destination while defending against Willie's detection.

3.1 Related work

IRS/RIS is a flat surface composed of a large number of reconfigurable and low-cost passive reflective elements, each of which is capable of controlling the phase and amplitude of the incident signal for optimal reflection, making the wireless channel between the transmitter and receiver more favorable for communication [24]. Following [23], several IRS/RIS-aided covert communication approaches have been developed. The authors in [25] considered the design of a latency-constrained covert RIS-assisted communication system when with the global CSI and without Willie's instantaneous CSI, respectively. The authors examined RIS-assisted covert communications by considering only Willie's statistical CSI is available [26]. The authors of [27] investigated the multiple-input-multiple-output (MIMO) covert communication assisted by RIS, where the covert rate was maximized by jointly designing the transmit covariance matrix and phase shift matrix. In [28], the authors proved that the reliability of communication transmission can be improved by adding RIS elements. Under the assumption that the number of channels used is infinite, the influence of AN on IRS-assisted covert communication is studied [29]. The authors in [30] adopted a two-way relaying protocol in the full-duplex relaying network assisted by RIS to realize covert communication. In [31], the authors studied the covert beamforming design of the IoT network assisted by the RIS. The information freshness maximization problem in IRS-aided full-duplex covert communications was studied in [32], where the non-retransmission protocol and the automatic repeat-request (ARQ) protocol are considered. In [33], UAV and IRS are combined to improve covert communication performance.

It should be emphasized that the existing studies on RIS-assisted covert communication all adopted fully-passive beamforming. In traditional RIS-assisted covert communication, due to the "double fading" effect of RIS, it's gain for covert performance is small [34], and the passive reflection of RIS limits the freedom of beamforming. The traditional RIS can be easily outperformed by a half-duplex relay when the number of elements in the RIS is not sufficiently large. Motivated by this, if a few passive elements of the IRS/RIS are replaced by active ones, the gain from active relaying can be achieved. The idea is to activate some elements of the RIS by connecting them to radio frequency (RF) chains and power amplifiers. This implies that if a few passive elements of the RIS are replaced by active ones, such that the traditional IRS becomes a hybrid relay-reflecting intelligent surface (HR-RIS) [35]. The active elements can not only modify the phase but also amplify the incident signal, improving the degrees of freedom in the beamforming. However, the amplitude of the passive element is generally set to 1, which means that it can only adjust the phase of the incident signal. HR-RIS requires extra cost in hardware implementation of active elements and signal processing. However, these only require a single or several active elements. Hardware and computing costs increase only slightly, given that the total number of elements in a traditional RIS is very large. It is not difficult to find that the active beamforming in HR-RIS is similar to the relay.

In HR-RIS-assisted covert communications, the reconfigurability of HR-RIS can be used to establish a favorable environment to enhance the quality of legitimate communications. Besides, the passive elements do not use a transmitter module, which incurs no additional power consumption and hardware cost compared with existing technologies based on active elements [36]. The active elements exploit the extra power consumption to overcome the "double-fading" effect. Compared to the AF relay, active elements utilize the principle of electromagnetic scattering to amplify signals directly, without the RF chain. Furthermore, HR-RIS works in FD mode without self-interference elimination.

In this paper, we consider covert communication from a transmitter (Alice) to a receiver (Bob) with the help of HR-RIS. In order to help Bob realize the low probability of being detected by Willie and improve the covert rate, an alternate optimization method was proposed to obtain the optimal reflection coefficient and transmit power. Our novelty is summarized as follows:

(1) We propose covert communication assisted by HR-RIS. The HR-IRS only needs to activate one or more elements of the IRS to act as an active relay. In this system, we consider the maximization of Bob's (covert user) covert rate under the covert constraint and total power constraint. For obtaining an efficient solution, matrix decomposition is used to deal with the non-convexity of the problem. On this basis, an alternating optimization (AO) method is proposed to obtain the optimal reflection phase shift of HR-IRS.
(2) Considering covert communication with finite block length, we used the Kullback-Leibler (KL) divergence on Willie as the covert constraint. In this case, the closed-form expression of the covertness

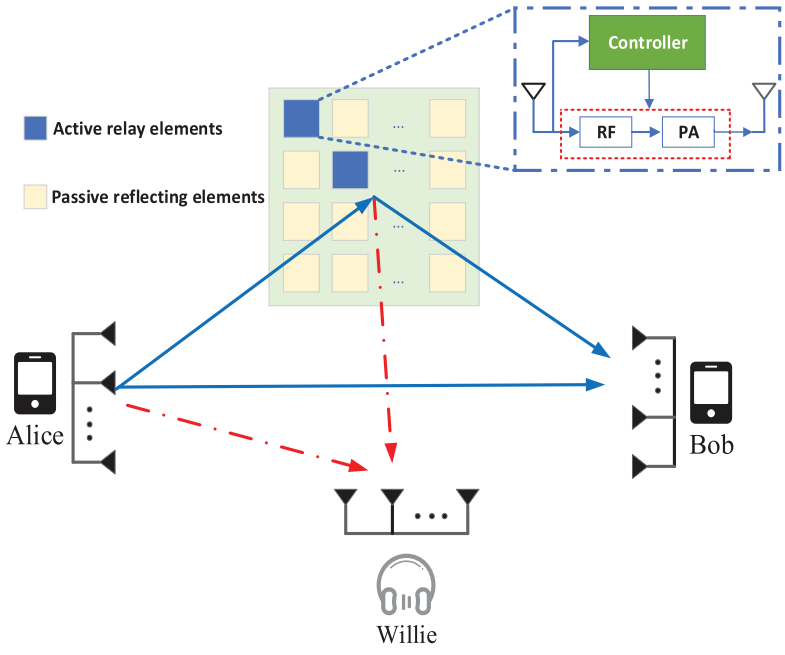

Figure 2. HR-RIS aided covert communication

constraint is derived, and it is proved that the KL divergence used in the covertness constraint is a monotonically increasing function of Willie's received power, based on which the optimal transmit power of Alice is obtained.

(3) We evaluate the performance of the proposed HR-IRS-assisted covert communication through simulations. Particularly, it shows that having a small number of active elements in the HR-IRS can significantly improve the achievable covert rate. In addition, compared with traditional IRS/RIS-assisted covert communication systems, our proposed system can obtain a large amount of covert rate gain.

3.2 Proposed HR-RIS assisted covert communication

As shown in Fig. 2, we propose a covert communication transmission scheme assisted by HR-RIS, where a transmitter (Alice) intends to send confidential information to a legitimate receiver (Bob) with the aid of the HR-RIS, while a warden (Willie) attempts to detect the existence of this transmission. There are two paths from Alice to Bob, *i.e.*, one is the direct link, and the other is the reflection/relaying link via HR-RIS. Similarly, there are also two paths from Alice to Willie. In addition, it is assumed that the signals reflected by the HR-RIS twice or more are ignored due to the significant path loss.

Alice, Bob, and Willie are assumed to be equipped with N_a, N_b, and N_w antennas, respectively. The HR-RIS is assumed to be equipped with N elements, including M passive reflecting elements and K active relaying elements (*i.e.*, $M + K = N$). The passive reflecting elements are implemented by a phase shifter, while the active relaying elements can tune the phase and amplitude of the incident signal. We assume that the active elements work in the AF mode. Therefore, for $K = 0$, HR-RIS returns to the traditional RIS. For $K = N$, by contrast, it becomes a relay station equipped with N antennas. Hence, in this work, we have $1 \leq K \leq N$. Furthermore, similar to the conventional RIS, we assume that each (active/passive) element of HR-RIS can independently reflect the received signals.

For the HR-RIS, $\mathbb{Q}$ represents the set of active relay elements. We define $\mathbf{\Theta} = \mathbf{\Phi} + \mathbf{\Psi}$, where $\mathbf{\Theta} = \text{diag}\{\theta_1, \ldots, \theta_N\} \in \mathbb{C}^{N\times N}$, $\mathbf{\Phi} = \text{diag}\{\phi_1, \ldots, \phi_N\} \in \mathbb{C}^{N\times N}$, and $\mathbf{\Psi} = \text{diag}\{\psi_1, \ldots, \psi_N\} \in \mathbb{C}^{N\times N}$, where $\mathbf{\Phi}$ and $\mathbf{\Psi}$ denote the reflection coefficients of passive elements and active elements, respectively. Therefore,

we have

$$\theta_n = \begin{cases} |\beta_n| e^{j\mu_n}, & \text{if} \quad n \in \mathbb{Q}, \\ e^{j\mu_n}, & \text{otherwise}, \end{cases} \tag{1}$$

where $\mu_n \in [0, 2\pi)$ represents the phase shift. We notice that $|\beta_n| = 1$ for $n \notin \mathbb{Q}$, and $|\beta_n|$ for $n \in \mathbb{Q}$ is determined by the total power of the active elements, which will be discussed later.

3.2.1 Transmission from Alice to Bob

When Alice transmits a confidential message, the received signal at Bob is given by

$$\begin{aligned} \mathbf{y}_b &= \sqrt{P_a}\mathbf{H}_{rb}\mathbf{\Psi}\mathbf{H}_{ar}\mathbf{x} + \sqrt{P_a}\mathbf{H}_{rb}\mathbf{\Phi}\mathbf{H}_{ar}\mathbf{x} + \sqrt{P_a}\mathbf{H}_{ab}\mathbf{x} + \mathbf{H}_{rb}\mathbf{\Psi}\mathbf{n}_r + \mathbf{n}_b \\ &= \sqrt{P_a}(\mathbf{H}_{rb}\mathbf{\Theta}\mathbf{H}_{ar} + \mathbf{H}_{ab})\mathbf{x} + \mathbf{n}_{bt}, \end{aligned} \tag{2}$$

where $\mathbf{n}_{bt} = \mathbf{H}_{rb}\mathbf{\Psi}\mathbf{n}_r + \mathbf{n}_b$ represents the total effective noise at the Bob. $\mathbf{H}_{ar}$ and $\mathbf{H}_{ab}$ are the steering vectors from Alice to HR-RIS and the steering vector from Alice to Bob, respectively, and $\mathbf{H}_{rb}$ denotes the steering vector from HR-RIS to Bob. In addition, $\mathbf{n}_r \sim \mathcal{CN}(\mathbf{0}, \sigma_r^2\mathbf{I}_K)$ and $\mathbf{n}_b \sim \mathcal{CN}(\mathbf{0}, \sigma_b^2\mathbf{I}_{N_b})$ are the complex additive white Gaussian noise (AWGN) space vectors at the K active elements of the HR-RIS and the Bob, respectively. For simplicity, we assume that $\sigma_r^2 = \sigma_b^2$ and $\mathbf{n}_{bt} \sim \mathcal{CN}(\mathbf{0}, \sigma_b^2(\mathbf{I}_{N_b} + \mathbf{H}_{rb}\mathbf{\Psi}\mathbf{\Psi}^H\mathbf{H}_{rb}^H))$. $\mathbf{x}$ is the signal vector transmitted by Alice, with each element following $\mathcal{CN}(0, 1)$, and P_a is Alice's transmit power, which should meet the constraint condition $P_a \leq P_a^{\max}$, where $P_a^{\max}$ is the maximum transmit power of Alice.

We assume that Bob's CSI is perfectly known by himself through channel estimation [37]. Following (2), Bob's covert rate in the HR-RIS-aided covert communication system can be expressed as [35]

$$f(\mathbf{\Theta}, P_a) = \log_2 |\mathbf{I}_{Nb} + \mathbf{\Omega}_b|, \tag{3}$$

where $\mathbf{\Omega}_b = P_a\mathbf{U}_b\mathbf{R}^{-1}/\sigma_b^2$, the signal covariance matrix is given by $\mathbf{U}_b = (\mathbf{H}_{rb}\mathbf{\Theta}\mathbf{H}_{ar} + \mathbf{H}_{ab})(\mathbf{H}_{rb}\mathbf{\Theta}\mathbf{H}_{ar} + \mathbf{H}_{ab})^H$, and the aggregate noise covariance matrix is given by $\mathbf{R} = (\mathbf{I}_{N_b} + \mathbf{H}_{rb}\mathbf{\Psi}\mathbf{\Psi}^H\mathbf{H}_{rb}^H) \in \mathbb{C}^{N_b \times N_b}$.

The transmit power of the active elements at the HR-RIS can be expressed as

$$P_r = \mathrm{Tr}(\mathbf{\Psi}(\mathbf{H}_{rb}\mathbf{H}_{rb}^H P_a + \sigma_b^2)\mathbf{\Psi}^H), \tag{4}$$

which should meet the constraint condition $P_r \leq P_r^{\max}$, where $P_r^{\max}$ is the maximum transmit power of all the K active elements.

3.2.2 Binary hypothesis testing at Willie

In this work, we focus on delay-constrained covert communication, that is, the number of channel uses L is finite. In order to detect the existence of a transmission, Willie attempts to distinguish the following two hypotheses:

$$\mathbf{y}_w = \begin{cases} \mathbf{n}_w, & \mathcal{H}_0, \\ \sqrt{P_a}(\mathbf{H}_{rw}\mathbf{\Theta}\mathbf{H}_{ar} + \mathbf{H}_{aw})\mathbf{x} + \mathbf{H}_{rw}\mathbf{\Psi}\mathbf{n}_r + \mathbf{n}_w, & \mathcal{H}_1, \end{cases} \tag{5}$$

where $\mathbf{H}_{aw}$ and $\mathbf{H}_{rw}$ are the steering vector from Alice to Willie and the steering vector from HR-RIS to Willie, respectively, and $\mathbf{n}_w \sim \mathcal{CN}(\mathbf{0}, \sigma_w^2\mathbf{I}_{N_w})$ is the AWGN space vector at Willie. $\mathcal{H}_0$ denotes the null hypothesis in which Alice does not transmit, and $\mathcal{H}_1$ denotes the alternative hypothesis where Alice transmits signals. Similarly, we assume that $\sigma_w^2 = \sigma_r^2$. Therefore, the total noise power at Willie is $\mathbf{n}_{wt} = (\mathbf{H}_{rw}\mathbf{\Psi}\mathbf{n}_r + \mathbf{n}_w) \sim \mathcal{CN}(\mathbf{0}, \sigma_w^2(\mathbf{I}_{N_w} + \mathbf{H}_{rw}\mathbf{\Psi}\mathbf{\Psi}^H\mathbf{H}_{rw}^H))$ under $\mathcal{H}_1$.

Considering the worst-case scenario for covert communication, we assume that Willie knows the channels perfectly. In this case, Willie has the maximum detection probability, and the corresponding covert performance can be used as a lower bound. In practice, the covert performance will be better than

or equal to the worst case. The probability density function of $\mathbf{y}_w$ under $\mathcal{H}_0$ and $\mathcal{H}_1$ can be respectively given by

$$\begin{aligned} f(\mathbf{y}_w|\mathcal{H}_0) &= \mathcal{CN}(\mathbf{0}, \sigma_w^2 \mathbf{I}_{N_w}), \\ f(\mathbf{y}_w|\mathcal{H}_1) &= \mathcal{CN}(\mathbf{0}, P_a \mathbf{U}_w + \sigma_w^2 (\mathbf{I}_{N_w} + \mathbf{H}_{rw} \mathbf{\Psi} \mathbf{\Psi}^H \mathbf{H}_{rw}^H)), \end{aligned} \tag{6}$$

where $\mathbf{U}_w = (\mathbf{H}_{rw} \mathbf{\Theta} \mathbf{H}_{ar} + \mathbf{H}_{aw})(\mathbf{H}_{rw} \mathbf{\Theta} \mathbf{H}_{ar} + \mathbf{H}_{aw})^H$.

Based on (6), the optimal detection threshold and the corresponding minimum detection error rate ξ^* at Willie can be derived [38]. However, due to the expression for ξ^* involves an incomplete gamma function, which cannot be handled by subsequent analysis and design. In order to deal with this difficulty, we present a lower bound of ξ^*. which is given by [39]

$$\xi^* \geq 1 - \sqrt{\frac{1}{2} \mathcal{D}_{01}}, \tag{7}$$

where $\mathcal{D}_{01}$ is the Kullback-Leibler (KL) divergence from $\mathbb{P}_0$ to $\mathbb{P}_1$, which is given by [38]

$$\mathcal{D}_{01} = L \left[\ln(1 + \gamma_w) - \frac{\gamma_w}{1 + \gamma_w} \right], \tag{8}$$

where γ_w is the signal-to-interference-plus-noise ratio (SINR) at Willie under $\mathcal{H}_1$ is given by

$$\gamma_w = \frac{|\mathbf{U}_w| P_a}{(|\mathbf{M}| \sigma_w^2)}, \tag{9}$$

where $\mathbf{M} = (\mathbf{I}_{N_w} + \mathbf{H}_{rw} \mathbf{\Psi} \mathbf{\Psi}^H \mathbf{H}_{rw}^H)$. We note that $\mathbf{U}_w$ and $\mathbf{M}$ are Hermitian matrices. Then, we perform the eigenvalue decomposition (EVD) on the above two matrices, which can be written as $\mathbf{U}_w = \mathbf{G} \mathbf{\Xi} \mathbf{G}^{-1}$ and $\mathbf{M} = \mathbf{J} \mathbf{\Lambda} \mathbf{J}^{-1}$, where $\mathbf{G}$ and $\mathbf{J}$ are matrices of eigenvectors of $\mathbf{U}_w$ and $\mathbf{M}$, respectively, and $\mathbf{G}$ and $\mathbf{J} \in \mathbb{C}^{N_w \times N_w}$, $\mathbf{\Xi} = \text{diag}\{\omega_1, \omega_2, \ldots, \omega_{N_w}\}$, ω_n is the nth eigenvalue of $\mathbf{U}_w$, $\mathbf{\Lambda} = \text{diag}\{\kappa_1, \kappa_2, \ldots, \kappa_{N_w}\}$, κ_n is the n-th eigenvalue of $\mathbf{M}$. As such, we have $|\mathbf{U}_w| = \prod_{i=1}^{N_w} \omega_i$ and $|\mathbf{M}| = \prod_{i=1}^{N_w} \kappa_i$.

In covert communications, $\xi^* > 1 - \epsilon$ is generally adopted as the covertness constraint, where ϵ is a small value to determine the required covertness level. Therefore, according to (7) and (8), we obtained the covertness constraint of Willie, which can be rewritten as

$$\mathcal{D}_{01} \leq 2\epsilon^2. \tag{10}$$

3.2.3 Problem formulation and solution

In this part, we jointly design the transmit power at Alice and relay/reflection coefficients of the HR-RIS to maximize the covert rate at Bob subject to the covertness and other constraints, of which the optimization problem can be formulated as

$$\begin{aligned} (\text{P1}): &\max_{\mathbf{\Theta}, P_a} f(\mathbf{\Theta}, P_a), && \text{(11a)} \\ &\text{s.t. } \mathcal{D}_{01} \leq 2\epsilon^2, && \text{(11b)} \\ &\quad |\beta_n| = 1, \text{ for } n \notin \mathbb{Q}, && \text{(11c)} \\ &\quad P_a \leq P_a^{\max}. && \text{(11d)} \end{aligned}$$

Our goal is to maximize the covert rate at Bob by jointly designing P_a and $\mathbf{\Theta}$. We propose an alternating optimization algorithm to optimize P_a and $\mathbf{\Theta}$. Specifically, we first optimize $\mathbf{\Theta}$ for a given P_a, and the objective function is transformed into a form that is easy to handle. Then, we optimize P_a for a given $\mathbf{\Theta}$.

First, we randomly generate the coefficient of HR-RIS and use $\mathcal{D}_{01} = 2\epsilon^2$ to get feasible P_a. The objective function $f(\mathbf{\Theta}, P_a)$ is non-convex with respect to $\mathbf{\Theta}$. In addition, the feasible set of (P1) is

non-convex due to the unit-modulus constraint (11c). Therefore, (P1) is difficult to be tackled. Thus, we approximate the objective function $f(\mathbf{\Theta}, P_a)$ by using its upper bound $f_0(\mathbf{\Theta}, P_a)$, which can be written as

$$\begin{aligned} f(\mathbf{\Theta}, P_a) &= \log_2 \left| \mathbf{I}_{N_b} + \frac{P_a \mathbf{U}_b \mathbf{R}^{-1}}{\sigma_b^2} \right| \\ &= \log_2 |\mathbf{R} + \rho \mathbf{U}_b| - \log_2 |\mathbf{R}| \\ &\overset{a}{\leq} \log_2 |\mathbf{R} + \rho \mathbf{U}_b| \\ &= \log_2 \left| \mathbf{R} + \rho (\mathbf{H}_{rb} \mathbf{\Theta} \mathbf{H}_{ar} + \mathbf{H}_{ab})(\mathbf{H}_{rb} \mathbf{\Theta} \mathbf{H}_{ar} + \mathbf{H}_{ab})^H \right| \\ &= f_0(\mathbf{\Theta}, P_a), \end{aligned} \tag{12}$$

where $\rho = P_a/\sigma_b^2$ and a is achieved by set $\mathbb{Q} = \emptyset$. We note that this upper bound becomes tighter as $\log_2 |\mathbf{R}|$ decreases.

Generally, the proposed solution is a sequential procedure where in each iteration, a specific coefficient of HR-RIS is updated when the others are fixed. Specifically, we let $\mathbf{a}_n^H \in \mathbb{C}^{N_b \times 1}$ denote the n-th row of $\mathbf{H}_{ab}$, and $\mathbf{b}_n \in \mathbb{C}^{N_b \times 1}$ denote the n-th column of $\mathbf{H}_{rb}$, *i.e.*, $\mathbf{H}_{ar} = [\mathbf{a}_1, \mathbf{a}_2, \ldots, \mathbf{a}_N]^H$, and $\mathbf{H}_{rb} = [\mathbf{b}_1, \mathbf{b}_2, \ldots, \mathbf{b}_N]$. Since $\mathbf{\Psi}$ and $\mathbf{\Theta}$ are diagonal matrices, we have $\mathbf{H}_{rb} \mathbf{\Theta} \mathbf{H}_{ar} = \sum_{n=1}^{N} \theta_n \mathbf{b}_n \mathbf{a}_n^H$ and $\mathbf{H}_{rb} \mathbf{\Psi} = \sum_{n \in \mathbb{Q}} \theta_n \mathbf{b}_n$. Hence, we can rewrite $f_0(\mathbf{\Theta}, P_a)$ as

$$\begin{aligned} f_0(\mathbf{\Theta}, P_a) &= \log_2 \left| \mathbf{R} + \rho (\mathbf{H}_{rb} \mathbf{\Theta} \mathbf{H}_{ar} + \mathbf{H}_{ab})(\mathbf{H}_{rb} \mathbf{\Theta} \mathbf{H}_{ar} + \mathbf{H}_{ab})^H \right| \\ &= \log_2 \Big| \mathbf{I}_{N_b} + \sum_{i \in Q} \theta_i \mathbf{b}_i \theta_i^* \mathbf{b}_i^H + \rho \sum_{i=1}^{N} |\theta_i|^2 \mathbf{b}_i \mathbf{a}_i^H \mathbf{a}_i \mathbf{b}_i^H \\ &+ \rho \mathbf{H}_{ab} \mathbf{H}_{ab}^H + \rho \sum_{i=1}^{N} \sum_{j=1, j \neq i}^{N} \theta_i \theta_j^* \mathbf{b}_i \mathbf{a}_i^H \mathbf{a}_j \mathbf{b}_j^H \\ &+ \rho \sum_{i=1}^{N} (\mathbf{H}_{ab} \theta_i^* \mathbf{a}_i \mathbf{b}_i^H + \theta_i \mathbf{b}_i \mathbf{a}_i^H \mathbf{H}_{ab}^H) \Big|. \end{aligned} \tag{13}$$

The objective function $f_0(\mathbf{\Theta}, P_a)$ can be rewritten as

$$\begin{aligned} f_0(\mathbf{\Theta}, P_a) &= \log_2 \left| \mathbf{A}_n + |\theta_n|^2 \mathbf{B}_n + \theta_n \mathbf{C}_n + \theta_n^* \mathbf{C}_n^H \right| \\ &= \log_2 |\mathbf{A}_n| + f_1(\mathbf{\Theta}, P_a), \end{aligned} \tag{14}$$

where $\mathbf{A}_n, \mathbf{B}_n, \mathbf{C}_n$ are obtained by some transformation.

Since $\mathbf{A}_n$ is an invertible matrix satisfying $\text{rank}(\mathbf{A}_n) = N_b$. Moreover, $\log_2(|\mathbf{A}_n|)$ is a constant, and $f_1(\mathbf{\Theta}, P_a)$ is given by

$$f_1(\mathbf{\Theta}, P_a) = \log_2 \left| \mathbf{I}_{N_b} + |\theta_n|^2 \mathbf{A}_n^{-1} \mathbf{B}_n + \theta_n \mathbf{A}_n^{-1} \mathbf{C}_n + \theta_n^* \mathbf{A}_n^{-1} \mathbf{C}_n^H \right|.$$

Similarly, the relationship between the transmit power of the relay and $\mathbf{\Psi}$ can be determined as

$$\begin{aligned} P_r &= \text{Tr}(\mathbf{\Psi}(\mathbf{H}_{rb} \mathbf{H}_{rb}^H P_a + \sigma_b^2) \mathbf{\Psi}^H) \\ &= P_a \sum_{n \in \mathbb{Q}} |\psi_n|^2 ||\mathbf{b}_n||^2 + \sigma_b^2 \sum_{n \in \mathbb{Q}} |\psi_n|^2 \\ &= \sum_{n \in \mathbb{Q}} |\psi_n|^2 [P_a ||\mathbf{b}_n||^2 + \sigma_b^2]. \end{aligned} \tag{15}$$

Denote $\widetilde{P}_r = \sum_{i \in \mathbb{Q}, i \neq n} |\psi_i|^2 [\sigma_b^2 + P_a ||\mathbf{b}_n||^2]$, which is a constant due to that the variables $\sum_{i \in \mathbb{Q}, i \neq n} \psi_i$ are fixed. Therefore, (15) can be rewritten as

$$\begin{aligned} P_r &= \sum_{n \in \mathbb{Q}} |\psi_n|^2 [P_a ||\mathbf{b}_n||^2 + \sigma_b^2] + \widetilde{P}_r \\ &= \sum_{n \in \mathbb{Q}} |\beta_n|^2 [P_a ||\mathbf{b}_n||^2 + \sigma_b^2] + \widetilde{P}_r. \end{aligned} \tag{16}$$

Here, we notice that $|\psi_n|^2 = |\beta_n|^2$ for $n \in \mathbb{Q}$.

Following the above, the problem of updating $\mathbf{\Theta}$, denoted by (P2), is given by

$$\begin{aligned} (\text{P2}): \max_{\mathbf{\Theta}} \ & f_1(\mathbf{\Theta}, P_a) && (17)\\ \mathbf{s.t.}\ & |\beta_n| = 1, && \text{for } n \notin \mathbb{Q},\\ & |\beta_n|^2 \le \frac{P_r^{\max} - \widetilde{P}_r}{[\sigma_b^2 + P_a||\mathbf{b}_n||^2]}, && \text{for } n \in \mathbb{Q}. \end{aligned}$$

In order to efficiently determine the optimal closed-form solution to (P2), the objective function $f_1(\mathbf{\Theta}, P_a)$ can be rewritten as

$$\begin{aligned} f_1(\mathbf{\Theta}, P_a) &= \log_2 |\mathbf{D}_n + \theta_n \mathbf{A}_n^{-1}\mathbf{C}_n + \theta_n^* \mathbf{A}_n^{-1}\mathbf{C}_n^H| \\ &= \log_2 |\mathbf{D}_n| + \log_2 |\mathbf{I}_{N_b} + \theta_n \mathbf{E}_n^{-1}\mathbf{C}_n + \theta_n^* \mathbf{E}_n^{-1}\mathbf{C}_n^H|, \end{aligned} \tag{18}$$

where $\mathbf{D}_n = \mathbf{I}_{N_b} + |\theta_n|^2 \mathbf{A}_n^{-1}\mathbf{B}_n$ and $\mathbf{E}_n = \mathbf{A}_n \mathbf{D}_n$.

We next analyse the objective function $f_1(\mathbf{\Theta})$ by considering the first term in (18), *i.e.*, $\log_2 |\mathbf{D}_n|$. Specifically, for $|\mathbf{D}_n|$, we note that $\text{rank}(\mathbf{A}_n^{-1}\mathbf{B}_n) < \text{rank}(\mathbf{B}_n) = 1$. Moreover, the probability of $\text{rank}(\mathbf{A}_n^{-1}\mathbf{B}_n)$ is close to zero (it only happens when $\mathbf{A}_n^{-1}\mathbf{B}_n = 0$). Thus, we have $\text{rank}(\mathbf{A}_n^{-1}\mathbf{B}_n) = 1$. Similarly, we find that $\mathbf{A}_n^{-1}\mathbf{B}_n$ is not diagonalizable when $\text{rank}(\mathbf{A}_n^{-1}\mathbf{B}_n) = 0$, which usually rarely happens. Based on this, we have $(\mathbf{A}_n^{-1}\mathbf{B}_n) \neq 0$ with a high probability and $\mathbf{A}_n^{-1}\mathbf{B}_n$ is diagonalizable. Hence, we can rewrite $\mathbf{A}_n^{-1}\mathbf{B}_n = \mathbf{W}_n \mathbf{\Sigma}_n \mathbf{W}_n^{-1}$ based on EVD, where $\mathbf{\Sigma}_n = \text{diag}\{\iota_n, 0, \ldots, 0\}$, ι_n is the only non-zero eigenvalue of $(\mathbf{A}_n^{-1}\mathbf{B}_n)$. Finally, since both $\mathbf{A}_n$ and $\mathbf{B}_n$ are positive semidefinite, ι_n is nonnegative and real. Thus, we have

$$\log_2 |\mathbf{D}_n| = \log_2 \left|1 + |\theta_n|^2 \iota_n\right|, \tag{19}$$

where ι_n is the only non-zero eigenvalue of $\mathbf{A}_n^{-1}\mathbf{B}_n$.

We are now focusing on the second term of (18). Thus, we have $\mathbf{E}_n^{-1}\mathbf{C}_n = \mathbf{T}_n \mathbf{\Gamma}_n \mathbf{T}_n^{-1}$ based on the EVD, where $\mathbf{T}_n \in \mathbb{C}^{N_b \times N_b}$, $\mathbf{\Gamma}_n = \text{diag}\{\lambda_n, 0, \ldots, 0\}$, λ_n is the sole non-zero eigenvalue of $\mathbf{E}_n^{-1}\mathbf{C}_n$. Let $\mathbf{V}_n = \mathbf{T}_n \mathbf{A}_n \mathbf{T}_n^{-1}$, and v_n denote first element of the first column of $\mathbf{V}_n^{-1}$ and $v_n^{'}$ denote first element of the first row of $\mathbf{V}_n$. Note that it follows that $v_n^{'} v_n = 1$. So, according to the [40], we can write

$$\log_2 |\mathbf{I}_{N_b} + \theta_n \mathbf{E}_n^{-1}\mathbf{C}_n + \theta_n^* \mathbf{E}_n^{-1}\mathbf{C}_n^H| = \log_2 (1 + |\theta_n|^2 |\lambda_n|^2 + 2\mathbb{R}(\theta_n \lambda_n) - v_n^{'} v_n |\lambda_n|^2), \tag{20}$$

where $\mathbb{R}$ denotes the real part of a complex number. We note that the additional coefficient $|\theta_n|^2$ is related to the active relay elements in HR-RIS, which does not exist in traditional RIS.

In summary, based on (19) and (20), we have

$$f_1(\mathbf{\Theta}, P_a) = \log_2 (1 + |\theta_n|^2 \iota_n) + \log_2 (1 + |\theta_n|^2 |\lambda_n|^2 + 2\mathbb{R}(\theta_n \lambda_n) - v_n^{'} v_n |\lambda_n|^2). \tag{21}$$

Hence, according to (21) we have $\mu_n^* = \arg(\lambda_n)$. So the optimal solution of the problem (P2) is given by

$$\theta_n^* = \begin{cases} |\beta_n| e^{-j\arg(\lambda_n)}, & n \in \mathbb{Q}, \\ e^{-j\arg(\lambda_n)}, & n \notin \mathbb{Q}. \end{cases} \tag{22}$$

In the HR-RIS, $\mathbb{Q}$ is available to determine $\{|\beta_n|\}_{n \in \mathbb{Q}}$. Therefore, from (P2), we obtain

$$|\beta_n| = \sqrt{\frac{P_r^{\max} - \widetilde{P}_r}{[\sigma_b^2 + P_a||\mathbf{b}_n||^2]}}, \quad n \in \mathbb{Q}. \tag{23}$$

As a result, the optimal solution to (P2) is given as

$$\theta_n^* = \begin{cases} \sqrt{\frac{P_r^{\max} - \widetilde{P}_r}{[\sigma_b^2 + P_a||\mathbf{b}_n||^2]}} e^{-j\arg(\lambda_n)}, & n \in \mathbb{Q}, \\ e^{-j\arg(\lambda_n)}, & n \notin \mathbb{Q}. \end{cases} \tag{24}$$

Remark 1. Substituting $\widetilde{P}_r = \sum_{i\in\mathbb{Q},i\neq n} |\beta_i|^2[\sigma_b^2 + P_a||\mathbf{b}_n||^2], n \in \mathbb{Q}$ to (23), it is observed that a larger K results in a smaller $|\beta_n|$. Therefore, increasing the number of active elements (*i.e.*, K) does not always guarantee the covert rate improvement of HR-RIS over traditional IRS. In particular, with a limited power budget $P_r^{\max}$, the HR-RIS can have $|\beta_n| < 1$, which attenuates the signal and degrades the covert rate. In this case, HR-RIS with a smaller K is more likely to attain a covert rate gain than those with more active elements. This conclusion will be further demonstrated numerically.

For a given $\mathbf{\Theta}$, we proved that the KL divergence adopted in the covertness constraint is a monotonically increasing function of the transmit power at Alice. Based on this, we can find the optimal transmit power of Alice P_a^* by solving $\mathcal{D}_{01} = 2\epsilon^2$. According to ((11)d), $P_a^* = \min(P_a, P_a^{\max})$ is the global optimal solution. Take P_a^* into (23) to get the amplitude coefficient of the optimized HR-RIS.

The details of the process are shown in Algorithm 1.

Algorithm 1 Find reflecting coefficients of the HR-RIS and transmit power

Input: $\mathbf{H}_{ar}$, $\mathbf{H}_{rb}$, $\mathbf{H}_{ab}$, $\mathbf{H}_{rw}$, $\mathbf{H}_{aw}$, $\mathbb{Q}$.
Output: $\{\theta_1^*, \theta_2^*, \ldots, \theta_N^*\}$, P_a^*.
Randomly generate a matrix θ_n where $|\beta_n| = 1$, $n \notin \mathbb{Q}$, and $\sum_{n\in\mathbb{Q}} |\beta_n|^2[P_a||\mathbf{b}_n||^2 + \sigma_b^2]$.
while The objective function does not converge **do**
  for $n = 1 \to N$ **do**
    Compute $\mathbf{A}_n$, $\mathbf{B}_n$, and $\mathbf{C}_n$.
    $\mathbf{D}_n = \mathbf{I}_{N_b} + |\theta_n|^2\mathbf{A}_n^{-1}\mathbf{B}_n$, $\mathbf{E}_n = \mathbf{A}_n\mathbf{D}_n$.
    Find λ_n as the sole non-zero eigenvalue of $\mathbf{E}_n^{-1}\mathbf{C}_n$.
    Update θ_n^* as (24).
  end for
end while
Find the optimal P_a^* based on $\mathcal{D}(\mathbb{P}_0|\mathbb{P}_1) = 2\epsilon^2$.
Update $|\beta_n|$ as (23).

Remark 2. According to (16), the amplitude of the active element will increase with its power, which increases the received power at Bob and Willie. Besides, from (8), when the covertness constraint satisfies $\mathcal{D}_{01} = 2\epsilon^2$, we can infer that the γ_w at Willie is a fixed value, therefore the transmit power should be decreased. In addition, the active element will amplify the noise at Willie and reduce γ_w, therefore, the transmit power will increase. Therefore, the increase in active power will cause a change in the transmit power.

The optimal number of active elements K can be solved by numerical search, which maximizes the objective function. From (16), for a given $P_r^{\max}$, the optimal number of active elements K can be solved by a one-dimensional bisection search over the interval $[1, N-1]$, where 1 and $N-1$ are the lower and upper bounds of the search interval. Given the accuracy 1, $N-1$ represents the number of elements that need to be compared by the bisection method, which means that the maximum iteration number is $(\log_2(N-1))$.

3.2.4 Convergence and complexity of the proposed algorithm

From Algorithm 1, we aim to find the unique non-zero eigenvalue of the matrix $\mathbf{E}_n^{-1}\mathbf{C}_n$. In each iteration, we find the unique non-zero eigenvalue of $\mathbf{E}_n^{-1}\mathbf{C}_n$ as a reflection coefficient of each HR-RIS element, so we can ensure that the objective function $f(\mathbf{\Theta}, P_a)$ is nondecreasing, defined as

$$f(\mathbf{\Theta}^{(t)}, P_a^{(t)}) \leq f(\mathbf{\Theta}^{(t)}, P_a^{(t+1)}) \leq f(\mathbf{\Theta}^{(t+1)}, P_a^{(t+1)}), \tag{25}$$

where $\mathbf{\Theta}^{(t+1)}$ and $P_a^{(t+1)}$ are the optimal solutions of HR-RIS and the optimal solutions of transmit power at the Alice. Therefore, the proposed AO algorithm monotonically converges to the local optimum of (P1) [41].

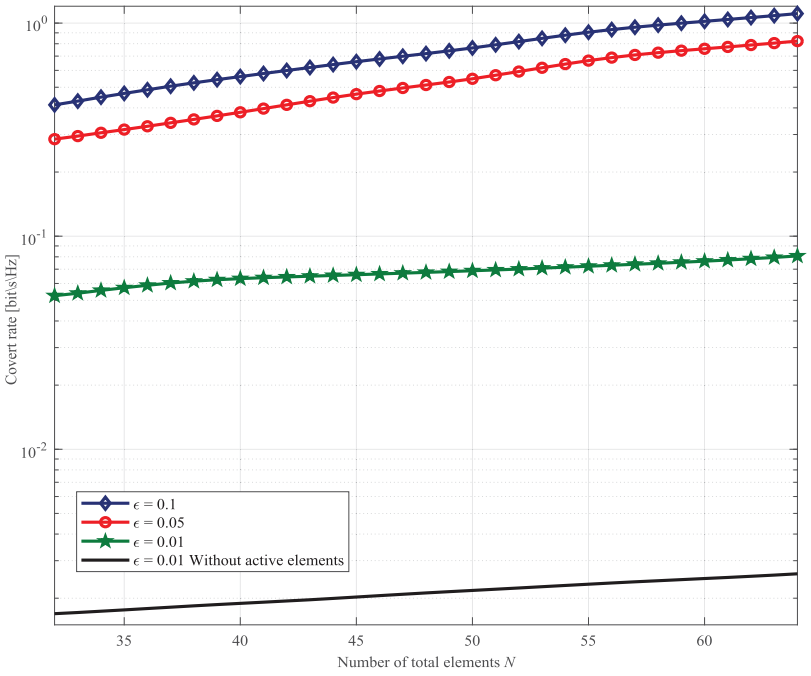

Figure 3. Covert rate *versus* the total number of reflecting elements at HR-RIS for different values of the covertness level ϵ, where $K = 3$, $P_r^{\max} = -30\,\text{dBm}$

3.2.5 The challenge to design a covert communication system by using the HR-RIS

In relay-assisted covert communication, it is generally only designed the relay beamforming vector aligns to Bob. In HR-RIS-assisted covert communication, the phase and amplitude of each element should be optimized, and the constant modulus constraint of passive elements is non-convex, improving the complexity of optimization. Compared with passive RIS, the active elements of HR-RIS will amplify the noise, which increases the design challenge of realizing covert transmission.

3.2.6 Numerical results

In Fig. 3, we plot the covert rate of Bob *versus* the total reflection elements N of the HR-RIS under different covert constraints ϵ. In this figure, we first observe that Bob's covert rate increases as N increases. We also note that for a given N, Bob's covert rate decreases as the ϵ decreases due to the fact that the covert constraint gets tighter. As expected, the figure illustrates that the use of active elements (i,e., $K = 3$) can achieve significant performance improvement with a higher covert rate at Bob compared with the traditional RIS, which demonstrates the benefits of introducing active elements to RIS in covert communications.

In Fig. 4, we investigate the covert rate *versus* the number of active elements K with different covert constraints. In this figure, it can be seen that Bob's covert transmission rate increases as K increases. For a small K, the HR-RIS performs far better than the RIS, even with a limited power budget. However, increasing K does not guarantee the covert rate improvement, especially for low $P_r^{\max}$, which is explained in Remark 1. As a result, when the maximum covert rate is obtained, we will not continue to increase the number of active elements K. Therefore, we can get the optimal number of active elements from this figure. Based on this, we can conclude that a small amount of active elements (*e.g.*, 5) is sufficient for HR-RIS to achieve a significant improvement in terms of the covert rate when compared to conventional IRS/RIS-aided covert communication schemes.

In Fig. 5, we investigate the covert rate *versus* the different distance between Alice and the IRS/HR-RIS X_r. For ease of comparison between different schemes, IRS and HR-RIS are assumed to be used in the same location. It can be observed that the optimal HR-RIS position to achieve the maximum covert rate is close to Bob (*i.e.*, (50 m, 2 m)), which is because the path loss from HR-RIS to Bob is small.

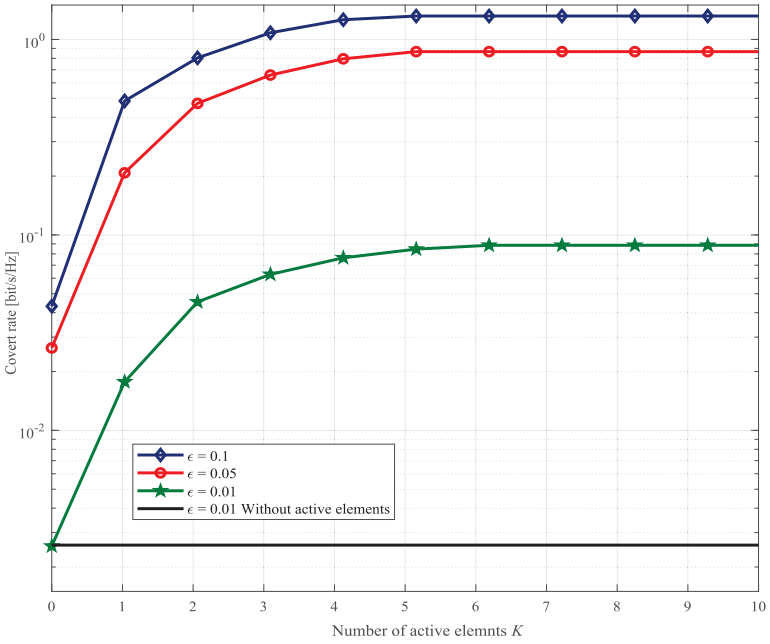

Figure 4. Covert rate *versus* the number of the active elements at the HR-RIS K for different values of the covertness level ϵ, where $N = 64$, $P_r^{\max} = -30\,\text{dBm}$

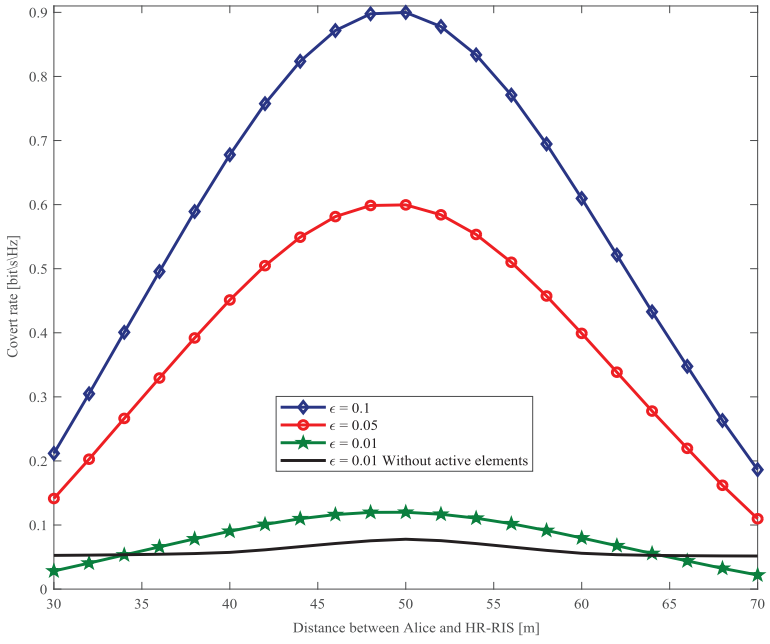

Figure 5. Covert rate *versus* different distance between Alice and the IRS/HR-RIS, where $N = 64$, $K = 2$, and $P_r^{\max} = -30\,\text{dBm}$

Likewise, this figure shows that the HR-RIS system with active components achieves a higher covert rate when compared to the traditional RIS scheme.

In Fig. 6, we plot the transmit power *versus* the active elements' power with different covertness constrains. From the figure, when $P_r^{\max}$ increases, the transmit power P_a will increase and approaches a limit value, which is explained in Remark 2. Therefore, employing active elements can use a higher transmit power to improve covert communication.

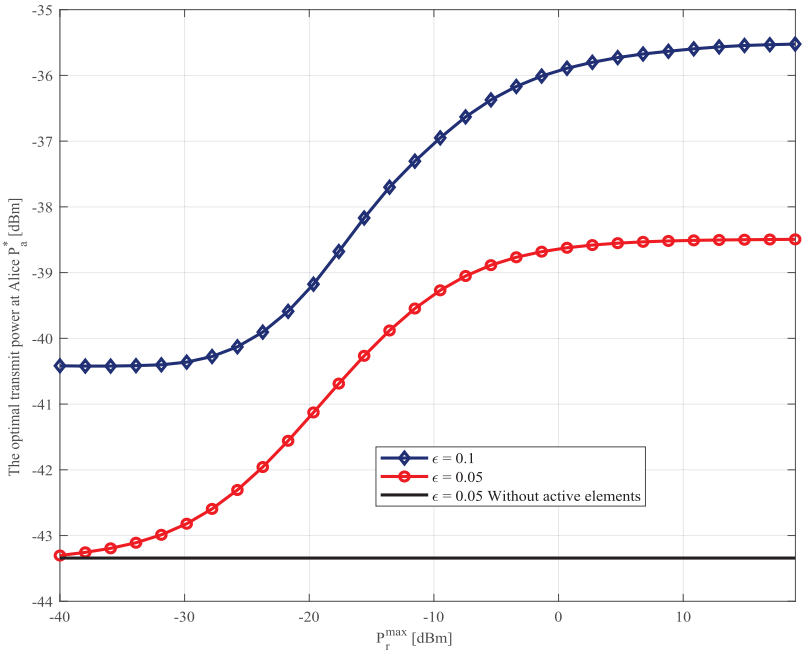

Figure 6. Transmit power *versus* the power of the active relay elements of the covertness level ϵ, where $K = 3$

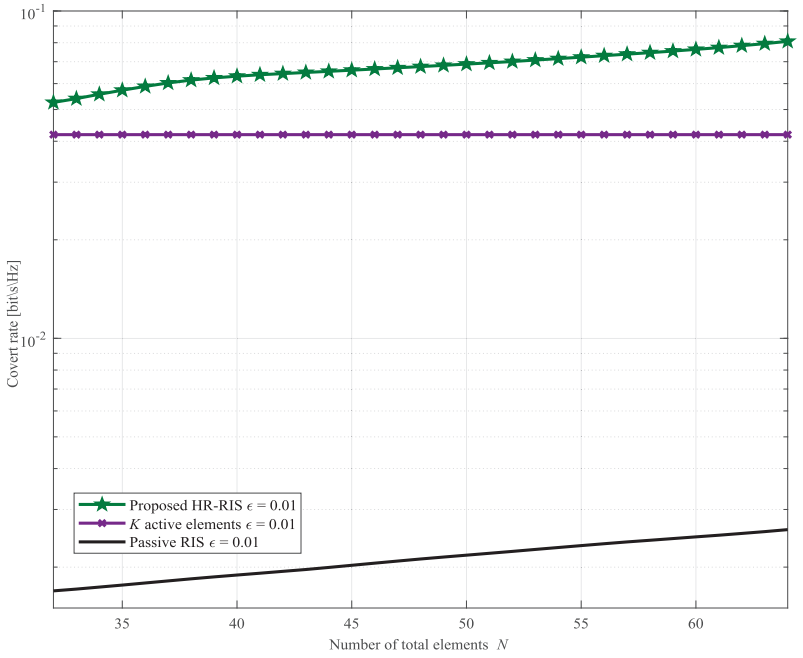

Figure 7. Covert rate *versus* different scheme with $\epsilon = 0.01$, $K = 3$ $P_r^{\max} = -30\,\mathrm{dBm}$

In Fig. 7, we plot the covert rate *versus* the number of total elements with different schemes, where $\epsilon = 0.01$, $K = 3$. From the figure, we can observe the active RIS is significantly better than the passive RIS, meanwhile, the performance of the proposed scheme is superior to that of the other two cases, which validates the effectiveness of our algorithm.

4 Conclusions

In this article, we first presented typical applications of relays in covert communication. Then, we proposed a covert communication scheme with the help of HR-RIS, where several elements are active elements, and the remaining ones as passive reflecting elements. We used KL divergence to represent Willie's detection performance, based on which, we obtained the optimal value of Alice's transmit power. Then, we used an alternating optimization algorithm to obtain the optimal reflection coefficients of HR-RIS to improve covert communication performance. The numerical results demonstrated that the proposed scheme significantly outperforms the conventional IRS/RIS-aided covert communication schemes in terms of covert rate by using a small number of active elements.

Conflict of Interest

The author declare no conflict of interest.

Data Availability

No data are associated with this article.

Authors' Contributions

Jinsong Hu mainly surveyed relay-assisted covert communication. Xiaoqiang Shi mainly surveyed covert communication assisted by hybrid relay-reflecting intelligent surfaces. Youjia Chen mainly surveyed the future challenges of HR-RIS-assisted covert communication and improved the readability of the paper by grammatical modification and polishing. Tiesong Zhao and Feng Shu designed the whole framework of the paper and the structure of the paper.

Acknowledgements

We thank the anonymous reviewers for their helpful comments.

Funding

This work was supported in part by the National Natural Science Foundation of China (Nos. 62001116, 62271150, 62171134, U22A2002 and 62071234), the Natural Science Foundation of Fujian Province under Grant (Nos.2020J05106 and 2022J01081), the Major Science and Technology plan of Hainan Province under Grant ZDKJ2021022, and the Scientific Research Fund Project of Hainan University under Grant KYQD(ZR)-21008.

References

[1] Yan S, Zhou X and Hu J, et al. Low probability of detection communication: Opportunities and challenges. IEEE Wireless Commun 2019; **26**: 19–25.
[2] Jiang X, Chen X and Tang J, et al. Covert communication in UAV-assisted air-ground networks. IEEE Wireless Commun 2021; **28**: 190–7.
[3] He B, Yan S and Zhou X, et al. On covert communication with noise uncertainty. IEEE Commun Lett 2017; **21**: 941–4.
[4] Wang D, Qi P and Zhao Y, et al. Covert wireless communication with noise uncertainty in space-air-ground integrated vehicular networks. IEEE Trans Intell Transp Syst 2022; **23**: 2784–97.
[5] Hu J, Yan S and Zhou X, et al. Covert communications without channel state information at receiver in IoT systems. IEEE Internet Things J 2020; **7**: 11103–14.
[6] Shahzad K and Zhou X. Covert wireless communications under quasi-static fading with channel uncertainty. IEEE Trans Inf Forensics Secur 2021; **16**: 1104–16.
[7] Cheng Z, Si J and Li Z, et al. Covert surveillance via proactive eavesdropping under channel uncertainty. IEEE Trans Commun 2021; **69**: 4024–37.
[8] Liu Z, Liu J and Zeng Y, et al. Covert wireless communications in IoT systems: Hiding information in interference. IEEE Wireless Commun 2018; **25**: 46–52.
[9] He B, Yan S and Zhou X, et al. Covert wireless communication with a poisson field of interferers. IEEE Trans Wireless Commun 2018; **17**: 6005–17.
[10] Cho KH and Lee SH. Treating interference as noise is optimal for covert communication over interference channels. IEEE Trans Inf Forensics Secur 2021; **16**: 322–32.
[11] Zheng T, Yang Z and Wang C, et al. Wireless covert communications aided by distributed cooperative jamming over slow fading channels. IEEE Trans Wireless Commun 2021; **20**: 7026–39.
[12] Shahzad K, Zhou X and Yan S, et al. Achieving covert wireless communications using a full-duplex receiver. IEEE Trans Wireless Commun 2018; **17**: 8517–30.
[13] Shu F, Xu T and Hu J, et al. Delay-constrained covert communications with a full-duplex receiver. IEEE Wireless Commun Lett 2019; **8**: 813–6.
[14] Shmuel O, Cohen A and Gurewitz O. Multi-antenna jamming in covert communication. IEEE Trans Commun 2021; **69**: 4644–58.
[15] Hu J, Yan S and Zhou X, et al. Covert wireless communications with channel inversion power control in rayleigh fading. IEEE Trans Veh Technol 2019; **68**: 12135–49.

[16] Hu J, Yan S and Zhou X, et al. Covert communication achieved by a greedy relay in wireless networks. IEEE Trans Wireless Commun 2018; **17**: 4766–79.
[17] Hu J, Yan S and Shu F, et al. Covert transmission with a self-sustained relay. IEEE Trans Wireless Commun 2019; **18**: 4089–102.
[18] Lv L, Li Z and Ding H, et al. Achieving covert wireless communication with a multi-antenna relay. IEEE Trans Inf Forensics Secur 2022; **17**: 760–73.
[19] Sun R, Yang B and Ma S, et al. Covert rate maximization in wireless full-duplex relaying systems with power control. IEEE Trans Commun 2021; **69**: 6198–212.
[20] Su Y, Sun H and Zhang Z, et al. Covert communication with relay selection. IEEE Wireless Commun Lett 2020; **10**: 421–5.
[21] Wang H, Zhang Y and Zhang X, et al. Secrecy and covert communications against UAV surveillance via multi-hop networks. IEEE Trans Commun 2019; **68**: 389–401.
[22] Sheikholeslami A, Ghaderi M and Towsley D, et al. Multi-hop routing in covert wireless networks. IEEE Trans Wireless Commun 2018; **17**: 3656–69.
[23] Lu X, Hossain E and Shafique T, et al. Intelligent reflecting surface enabled covert communications in wireless networks. IEEE Network 2020; **34**: 148–55.
[24] Wu Q and Zhang R. Beamforming optimization for wireless network aided by intelligent reflecting surface with discrete phase shifts. IEEE Trans Commun 2019; **68**: 1838–51.
[25] Zhou X, Yan S and Wu Q, et al. Intelligent reflecting surface (IRS)-aided covert wireless communications with delay constraint. IEEE Trans Wireless Commun 2021; **21**: 532–47.
[26] Wu C, Yan S and Zhou X, et al. Intelligent reflecting surface (IRS)-aided covert communication with warden's statistical CSI. IEEE Wireless Commun Lett 2021; **10**: 1449–53.
[27] Chen X, Zheng T and Dong L, et al. Enhancing MIMO covert communications via intelligent reflecting surface. IEEE Wireless Commun Lett 2021; **11**: 33–7.
[28] Wu Y, Wang S and Luo J, et al. Passive covert communications based on reconfigurable intelligent surface. IEEE Wireless Commun Lett 2022; **11**: 2445–9.
[29] Wang C, Li Z and Shi J, et al. Intelligent reflecting surface-assisted multi-antenna covert communications: Joint active and passive beamforming optimization. IEEE Trans Commun 2021; **69**: 3984–4000.
[30] Deng D, Li X and Dang S, et al. Covert communications in intelligent reflecting surface-assisted two-way relaying networks. IEEE Trans Veh Technol 2022; **71**: 12380–5.
[31] Ma S, Zhang Y and Li H, et al. Covert beamforming design for intelligent-reflecting-surface-assisted IoT networks. IEEE Internet Things J 2021; **9**: 5489–501.
[32] Wang C, Li Z and Zheng T, et al. Intelligent reflecting surface-aided full-duplex covert communications: Information freshness optimization. IEEE Trans Wireless Commun 2022.
[33] Wang C, Chen X and An J, et al. Covert communication assisted by UAV-IRS. IEEE Trans Commun 2022; **71**: 357–69.
[34] Najafi M, Jamali V and Schober R, et al. Physics-based modeling and scalable optimization of large intelligent reflecting surfaces. IEEE Trans Commun 2021; **69**: 2673–91.
[35] Nguyen NT, Vu QD and Lee K, et al. Hybrid relay-reflecting intelligent surface-assisted wireless communications. IEEE Trans Veh Technol 2022; **71**: 6228–44.
[36] Renzo MD, Debbah M and Phan-Huy DT, et al. Smart radio environments empowered by reconfigurable AI meta-surfaces: An idea whose time has come. EURASIP J Wireless Commun Networking 2019; **2019**: 1–20.
[37] Wang Z, Liu L and Cui S. Channel estimation for intelligent reflecting surface assisted multiuser communications: Framework, algorithms, and analysis. IEEE Trans Wireless Commun 2020; **19**: 6607–20.
[38] Yan S, He B and Zhou X, et al. Delay-intolerant covert communications with either fixed or random transmit power. IEEE Trans Inf Forensics Secur 2018; **14**: 129–40.
[39] Bash BA, Goeckel D and Towsley D. Limits of reliable communication with low probability of detection on AWGN channels. IEEE J Sel Areas Commun 2013; **31**: 1921–30.
[40] Zhang S and Zhang R. Capacity characterization for intelligent reflecting surface aided MIMO communication. IEEE J Sel Areas Commun 2020; **38**: 1823–38.
[41] Marks BR and Wright GP. A general inner approximation algorithm for nonconvex mathematical programs. Oper Res 1978; **26**: 681–3.

Jinsong Hu received his B.S. degree and Ph.D. degree from the School of Electronic and Optical Engineering, Nanjing University of Science and Technology, Nanjing, China in 2013 and 2018, respectively. From 2017 to 2018, he was a Visiting Ph.D. Student at the Research School of Engineering, Australian National University, Canberra, ACT, Australia. He is an associate professor at the College of Physics and Information Engineering, Fuzhou University, Fuzhou, China. He served as a TPC member for the IEEE ICC2020/2019. His research interests include array signal processing, covert communications, and physical layer security.

Xiaoqiang Shi received the B.S. degree from the School of Physics and Electronic Information Engineering, Minjiang University, Fuzhou, China, in 2020. He is pursuing his M.S. degree in College of Physics and Information Engineering, Fuzhou University, Fuzhou, China. His research interests include covert communication and intelligent reflecting surface.

Youjia Chen received the B.S. and M.S. degrees in communication engineering from Nanjing University, Nanjing, China, and Ph.D. degree in wireless engineering from the University of Sydney, Australia, in 2005, 2008 and 2017, respectively. Currently, she is a professor at the College of Physics and Information Engineering, Fuzhou University, China. She has published over 30 research papers in leading international journals and conference, and contributed to a Wiley-IEEE Press book. Her current research interests include wireless caching/computing, intelligent reflecting surfaces, internet of video things, and wireless AI.

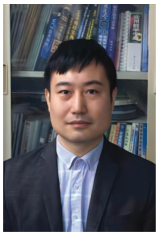

Tiesong Zhao received the B.S. degree in electrical engineering from the University of Science and Technology of China, Hefei, China, in 2006, and the Ph.D. degree in computer science from the City University of Hong Kong, Hong Kong, in 2011. He served as a Research Associate with the Department of Computer Science, City University of Hong Kong, from 2011 to 2012; a Postdoctoral Fellow with the Department of Electrical and Computer Engineering, University of Waterloo, from 2012 to 2013; and a Research Scientist with the Ubiquitous Multimedia Laboratory, The State University of New York at Buffalo, from 2014 to 2015. He is currently a Minjiang Distinguished Professor with the College of Physics and Information Engineering, Fuzhou University, China. He also works with the coding, quality assessment, and transmission. Due to his contributions in video coding and transmission, he received the Fujian Science and Multimedia Signal Processing Studio, Peng Cheng Laboratory, Shenzhen, China. His research interests include multimedia signal processing. Technology Award for Young Scholars in 2017. He has also been serving as an Associate Editor of IET Electronics Letters since 2019.

Feng Shu received the B.S. degree from Fuyang Teaching University, Fuyang, China, in 1994, the M.S. degree from Xidian University, Xi'an, China, in 1997, and the Ph.D. degree from Southeast University, Nanjing, China, in 2002. Since November 2020, he has been with the School of Information and Communication Engineering, Hainan University, where he is currently a Professor of the third level, and also a Supervisor of the Ph.D. students. From 2009 to 2010, he was a Post-Doctoral Researcher with The University of Texas at Dallas. He has published about 300 articles, of which over 200 are in archival journals, including more than 100 articles in the IEEE journals and more than 150 SCI-indexed articles. His research interests include wireless networks and array signal processing. He is currently recognized as a Plan of Leading Talents in Hainan Province. He was also the Mingjiang Chair Professor and a Hundreds-of-Talented Plan in Fujian Province. He is currently an Associate Editor of IEEE Systems Journal, IEEE Wireless Communications Letters, and IEEE Access.